Zero-core-contribution calculation of photodetachment cross sections of O_2^- and S_2^-

R. M. Stehman
Department of Physics, Northeastern Illinois University, Chicago, Illinois, 60625

S. B. Woo
Department of Physics, University of Delaware, Newark, Delaware, 19711

(Received 23 December 1980)

The zero-core-contribution model allows photodetachment cross sections to be computed using a few readily accessible input parameters. We apply this model to the computation of photodetachment cross sections for the homonuclear diatomic ions O_2^- and S_2^-, which have π_g outer orbitals. Values are calculated for the total cross sections, partial cross sections for each vibrational channel, and angular distributions for each vibrational channel. The results are in good agreement with experimental values. Inclusion of vibrational effects allows the prediction of total photodetachment cross sections as a function of ion vibrational temperature. This allows comparison with both swarm and beam-type experiments. The simplicity of the model makes it of use in the interpretation of experimental results. This is illustrated by applying the model to infer equilibrium internuclear distances. We obtain $r_e'' = 1.348$ Å for O_2^- and $r_e'' = 2.004$ Å for S_2^-. We anticipate that the simplicity of the model will allow its application to heteronuclear diatomic and polyatomic negative ions.

I. INTRODUCTION

In a recent article[1] we introduced a zero-core-contribution (ZCC) model for describing atomic negative ions. It allows one to calculate the photodetachment cross section of an atomic negative ion if the following three easily accessible parameters are known: (1) the angular momentum of the outermost orbital of the ion, (2) the electron affinity, and (3) the size of the parent neutral atom. In the present paper we extend this model to calculate the photodetachment cross sections of homonuclear diatomic negative ions. Although we deal specifically with ions of π_g symmetry (e.g., O_2^- and S_2^-), the treatment illustrates many of the points to be considered in the calculation of photodetachment cross sections of other types of diatomic and polyatomic negative ions.

There have been several experimental investigations of the energy dependence of the total photodetachment cross section of O_2^- using crossed ion-photon beams[2,3] and drift-tube techniques.[4-6] In addition, there have been measurements of the energy spectrum of the detached electrons [laser photoelectron spectroscopy (LPES) experiments][7,8] for O_2^- and S_2^-. These LPES experiments yield ratios of partial cross sections for photodetachment via different vibrational channels. The angular distribution of electrons detached from O_2^- has also been measured.[7] The ZCC model calculates the energy dependence of the total photodetachment cross section, partial cross sections, and angular distributions in agreement with these experiments. The ZCC calculations for individual vibrational channels, used in conjunction with the LPES data, provide an improved determination of the equilibrium internuclear distance in the O_2^- and S_2^- ions.

There are very few articles which give theoretical calculations of cross sections for detachment from any molecular ion. Geltman[9] derived the threshold behavior for detachment from a cylindrically symmetric system. A method for deriving the threshold behavior of polyatomic negative ions has been developed by Reed *et al.*,[10] whose work also presents what is apparently the first calculation of the cross section for photodetachment for any molecular negative ion. However, the work of Reed *et al.* does not incorporate the vibrational motion of the ion and molecule. It does not calculate the partial cross sections for individual vibrational and electronic channels, nor does it calculate the angular distribution of the detached electrons, in contrast to the present work.

The ZCC model depicts a negative ion as an equivalent one-electron system. The one electron, referred to as the "extra" electron, is bound by an effective short-range potential which is constant outside a core region. Its wave function is referred to as the "detachment orbital". The contribution to photodetachment owing to the extra electron's wave function inside the core region is assumed zero. Application of this model to the diatomic ions O_2^- and S_2^- requires knowledge of the following quantities: (1) the nature of the molecular orbital of the extra electron (this is known[11] to be π_g), (2) the vertical detachment energies corresponding to each vibrational transition contributing to the total cross section (in contrast, the same calculation for atomic negative ions requires only the electron affinity), (3) the size of the neutral atoms from which the ion is formed, and the equilibrium internuclear distance

 © 1981 The American Physical Society

of the ion, and (4) the internuclear potentials for the ion and molecule, from which the Franck-Condon factors for vibrational transitions can be calculated. The quantities needed for (2) and (3) are available from various sources. For the internuclear potentials we have assumed Morse potentials.

II. EXTENSION OF THE ZCC MODEL TO HOMONUCLEAR DIATOMIC IONS

A. Separation of the nuclear and electronic motion

We consider a photodetachment process corresponding to the transition from an initial state $\Phi_{i\nu''}$ of the ion to a final state $\Phi_{\vec{k}f\nu'}$ of the molecule and detached electron. The ion's electronic state is denoted by the index i, and the vibrational state of the ion by ν''. The momentum of the detached electron is denoted by $\vec{k}$, the electronic state of the molecule by f, and the vibrational state of the molecule by ν'. In this discussion, we make the simplifying assumption that the only effect of the rotational motion is to randomize the orientation of the ions.[12] Thus the cross section for detachment from a molecular ion will be related to the dipole matrix element

$$M(\vec{k},f,\nu',i,\nu'',\hat{m}) = \langle \Phi_{\vec{k}f\nu'} | d | \Phi_{i\nu''} \rangle , \tag{1}$$

where $\hat{m}$ is a unit vector parallel to the axis of the molecule. The dipole length operator is

$$d = \sum_{j=1}^{n+1} \hat{e} \cdot \vec{r}_j , \tag{2}$$

where $\hat{e}$ is a unit vector in the direction of polarization of the incident light and $\vec{r}_j$ is the position of the jth electron. In order to write d in the form of Eq. (2), we must choose a coordinate system with its origin at the midpoint of the internuclear axis. Otherwise d would contain the nuclear coordinates.

The Born-Oppenheimer approximation allows $\Phi_{i\nu''}$ and $\Phi_{f\nu''}$ to be factored:

$$\Phi_{i\nu''}(\vec{r}_1 \cdots \vec{r}_{n+1}, R) = \Psi_{iR}(\vec{r}_1 \cdots \vec{r}_{n+1}) \chi''_{\nu''}(R) \tag{3}$$

and

$$\Phi_{\vec{k}f\nu'}(\vec{r}_1 \cdots \vec{r}_{n+1}, R) = \Psi_{\vec{k}fR}(\vec{r}_1 \cdots \vec{r}_{n+1}) \chi'_{\nu'}(R) , \tag{4}$$

where R is the internuclear distance and $\chi''_{\nu''}(R)$ and $\chi'_{\nu'}(R)$ are the wave functions describing the vibrational motion of the ion and the molecule, respectively. $\Psi_{iR}(\vec{r}_1 \cdots \vec{r}_{n+1})$ is the wave function of the $n+1$ electrons of the ion, and $\Psi_{\vec{k}fR}(\vec{r}_1 \cdots \vec{r}_{n+1})$ is the wave function of the n electrons of the molecule plus a detached electron. Then

$$M(\vec{k},f,\nu',i,\nu'',\hat{m}) = \int \chi'_{\nu'}(R) \chi''_{\nu''}(R) M^e_{\vec{k}fi}(R,\hat{m}) dR , \tag{5}$$

where the electronic matrix element $M^e_{\vec{k}fi}(R,\hat{m})$ is

$$M^e_{\vec{k}fi}(R,\hat{m}) = \left\langle \Psi_{\vec{k}fR} \left| \sum_{j=1}^{n+1} \hat{e} \cdot \vec{r}_j \right| \Psi_{iR} \right\rangle . \tag{6}$$

It is convenient to expand $M^e_{\vec{k}fi}$ in a Taylor's series in R about an appropriate value $\bar{R}$. If $\bar{R}$ is chosen to be

$$\bar{R} = R_{\nu'\nu''} \equiv \frac{\int \chi'_{\nu'}(R) \chi''_{\nu''}(R) R\, dR}{\int \chi'_{\nu'}(R) \chi''_{\nu''}(R)\, dR} , \tag{7}$$

and terms of second and higher order in the Taylor's expansion are ignored,[13] $M(\vec{k},f,\nu',i,\nu'',\hat{m})$ can be written as a product

$$M(\vec{k},f,\nu',i,\nu'',\hat{m}) = M^e_{\vec{k}fi}(R_{\nu'\nu''},\hat{m}) \int \chi'_{\nu'}(R) \chi''_{\nu''}(R) dR . \tag{8}$$

The absolute square of the overlap integral of the vibrational wave functions in Eq. (8) is the well-known Franck-Condon factor

$$F(\nu',\nu'') = \left| \int \chi'_{\nu'}(R) \chi''_{\nu''}(R)\, dR \right|^2 . \tag{9}$$

$F(\nu',\nu'')$ does not depend on the orientation $\hat{m}$. Thus, using Fermi's golden rule, the cross section for detachment from a diatomic negative ion is

$$\frac{d\sigma}{d\Omega}(\vec{k},f,\nu',i,\nu'') = F(\nu',\nu'')(2\pi)^2 \frac{e^2}{\hbar c} \frac{m_e k \omega}{\hbar} \times \int |M^e_{\vec{k}fi}(R_{\nu'\nu''},\hat{m})|^2 \frac{d\Omega_m}{4\pi} , \tag{10}$$

where $e^2/\hbar c$ is the fine-structure constant, m_e is the mass of an electron, ω is the frequency of the incident light, and $d\Omega$ is an element of solid angle in the direction of the detached electron's momentum $\vec{k}$. $d\Omega_m$ is an element of solid angle of the vector $\hat{m}$. The integral over $d\Omega_m$ and the factor $1/4\pi$ yield a cross section which is averaged over all molecular orientations. The numerical factor in Eq. (10) assumes that the continuum final state is normalized such that

$$\langle \psi_{\vec{k}'fR} | \psi_{\vec{k}fR} \rangle = \delta(\vec{k} - \vec{k}') . \tag{11}$$

In particular, if the final state is a one-electron plane wave, this normalization gives

$$\psi_{\vec{k}}(\vec{r}) = \frac{1}{[(2\pi)^3]^{1/2}} e^{i\vec{k}\cdot\vec{r}} . \tag{12}$$

B. Reduction to the one-electron problem

The formula for the cross section, Eq. (10), uses a matrix element which connects $(n+1)$-electron wave functions. To see how the $(n+1)$-electron matrix element can be related to matrix ele-

ments connecting one-electron wave functions, we briefly outline the nature of the $(n+1)$-electron wave functions which lie behind the ZCC model. We consider only the outer-shell electrons of the anion. For O_2^-, there are three outer-shell electrons occupying π_g orbitals. We choose two of these orbitals to be undistorted orbitals of the neutral molecule. These two will henceforth be referred to as the molecular orbitals. The third orbital, which we call the detachment orbital, is chosen to describe the change in charge density in the region outside the neutral molecule owing to the extra electron. Therefore, the detachment orbital has a mathematical form distinct from that of the molecular orbitals. The detachment orbital will be denoted by ψ_λ, where the axial component of angular momentum $\lambda = \pm 1$ corresponding to a π_g orbital.

We require that the wave function of the three outer-shell electrons of the ion represents a state with axial component of total orbital angular momentum $\Lambda = \pm 1$ and z component of total spin $M_S = \pm\frac{1}{2}$. These states belong to the $^2\Pi_g$ ground electronic term[14] of O_2^-. We also require that this wave function is antisymmetric with respect to exchange of any pair of electrons. A wave function fulfilling these requirements can be constructed by combining the two molecular orbitals and the detachment orbital,[15] using the concept of fractional parentage.[16]

The final-state wave function is an antisymmetrized combination of the two molecular orbitals and a one-electron outgoing wave $\psi_{\vec{k}}$. The two molecular orbitals are combined, using standard methods,[17] to give one of the states of the $^3\Sigma_g^-$, $^1\Delta_g$, or $^1\Sigma_g^+$ electronic term of the molecule. The essential feature is that the same molecular orbitals are used in the initial- and final-state $(n+1)$-electron wave functions. The only one-electron functions which differ between the initial and final states are the detachment orbital ψ_λ, and the outgoing wave $\psi_{\vec{k}}$. Because of this, the matrix element $M^e_{\vec{k}fi}$ can be written as a factor times a one-electron matrix element

$$M_{\vec{k}\lambda}(R,\hat{m}) = \int \psi^*_{\vec{k}}(\vec{r})\hat{e}\cdot\vec{r}\,\psi_\lambda(\vec{r})\, r^2 \sin\theta\, d\phi\, d\theta\, dr\,, \quad (13)$$

plus terms which are multiplied by the overlap integral of ψ_λ with molecular orbitals.[17] We neglect these overlap terms since the ZCC model assumes the detachment orbital is zero in the region where the molecular orbitals dominate.

We will use the symbol (A,ν',ν'') to signify a channel beginning with the ion in the vibrational state ν'' and any of the four degenerate electronic states i belonging to the $^2\Pi_g$ electronic term. The channel leaves the molecule in the vibrational state ν' and one of the electronic states f belonging to the electronic term A. A represents either $^3\Sigma_g^-$, $^1\Delta_g$, or $^1\Sigma_g^+$. The cross section for detachment via this channel is obtained by averaging the cross section given in Eq. (10) over the states i, and summing over the final states f which belong to the term A. It can be shown[15] that

$$\frac{d\sigma}{d\Omega}(A,\nu',\nu'') = \tfrac{1}{4}\sum_i \sum_f \frac{d\sigma}{d\Omega}(\vec{k},f,\nu',i,\nu'')$$

$$= F(\nu',\nu'')(2\pi)^2 \frac{e^2}{\hbar c}\frac{m_e k\omega}{\hbar}\left|\langle A,\pi_g\}\,^2\Pi_g\rangle\right|^2$$

$$\times \tfrac{1}{2}\sum_{\lambda=\pm1}\left|M_{\vec{k}\lambda}(R_{\nu'\nu''},\hat{m})\right|^2 \frac{d\Omega_m}{4\pi}\,. \quad (14)$$

The fractional parentage coefficient $\langle A,\pi_g\}\,^2\Pi_g\rangle$ connects the parent electronic term A of the molecule and the π_g one-electron orbital with the $^2\Pi_g$ electronic term of the ion. It can be calculated from known formulas.[16]

Equation (14) is the formula used for computing photodetachment cross sections in this paper. It represents a one-electron approach in that it involves an average of the one-electron matrix element over the two orientations of the one-electron axial component of angular momentum, indicated by the factor $\frac{1}{2}$ times the sum over $\lambda = \pm 1$. It should be noted that if the initial multielectron wave function were built up using three identical outer-shell orbitals, all considered to participate in photodetachment, Eq. (14) would contain another factor of 3 on the right-hand side. This is in contrast to our method, employing a single detachment orbital and two molecular orbitals.

C. The single-electron wave functions

In order to represent the region occupied by a neutral diatomic molecule, we take the core region to be composed of two overlapping spheres. Each sphere has a radius chosen as in Ref. 1 for atomic negative ions:

$$r_0 = 1.3(\langle r^2\rangle)^{1/2}\,, \quad (15)$$

where $\langle r^2\rangle$ is the expectation value of r^2 for the outermost shell of the neutral atom. The distance between the centers of the spheres is the equilibrium internuclear distance of the ion. The overlapping spheres core region is illustrated in Fig. 1(a), drawn to scale for O_2^-. Figures 1(b) and 1(c) show alternative oval and ellipsoidal core shapes which also have cylindrical symmetry appropriate for a diatomic molecule.

Outside the core region, we choose ψ_λ to be a linear combination of p-atomic orbitals (LCAO):

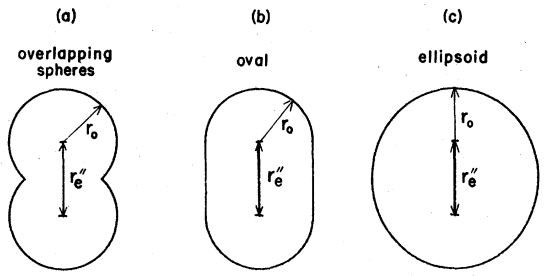

FIG. 1. Possible core shapes for homonuclear diatomic anions.

$$\psi_{\pm 1}=\frac{1}{\sqrt{2\pi}}e^{\pm i\varphi}f(r,\theta) \tag{16}$$

with

$$f(r,\theta)=N[\psi_p(r_A,\theta_A)-\psi_p(r_B,\theta_B)] \tag{17}$$

and

$$\psi_p(r,\theta)=\left(1+\frac{1}{\gamma r}\right)\frac{e^{-\gamma r}}{r}\sin\theta\,. \tag{18}$$

The spherical coordinates r_A and θ_A are measured relative to one nucleus, and r_B and θ_B are measured relative to the second nucleus. The normalization constant N in Eq. (17) is chosen such that

$$\int[f(r,\theta)]^2 r^2\sin\theta\,d\theta\,dr=1\,, \tag{19}$$

where the integration is only over values of r and θ lying outside the core. The negative sign between the two terms in Eq. (17) makes ψ_λ symmetric with respect to inversion of the spatial coordinates, which corresponds to gerade symmetry.

The LCAO wave function, as given in Eqs. (17) and (18) is not the only detachment orbital having the correct asymptotic behavior and corresponding to π_g symmetry. A mixed LCAO detachment orbital could be constructed, using p- and d-atomic orbitals, such that

$$f(r,\theta)=N[(1-\delta^2)^{1/2}f_p(r,\theta)+\delta f_d(r,\theta)]\,, \tag{20}$$

with

$$f_p(r,\theta)=N_p[\psi_p(r_A,\theta_A)-\psi_p(r_B,\theta_B)]\,, \tag{21}$$

where ψ_p is given by Eq. (18), and

$$f_d(r,\theta)=N_d[\psi_d(r_A,\theta_A)+\psi_d(r_B,\theta_B)]\,, \tag{22}$$

where

$$\psi_d=\left(1+\frac{3}{\gamma r}+\frac{3}{\gamma^2 r^2}\right)\frac{e^{-\gamma r}}{r}\sin\theta\cos\theta\,. \tag{23}$$

N_p, N_d, and N are chosen so that $f_p(r,\theta)$, $f_d(r,\theta)$, and $f(r,\theta)$ are normalized to unity outside the core region. Note $N\neq 1$ because of the overlap between f_p and f_d. δ is a parameter which establishes the amount and phase of the d orbitals in the linear combination. When $\delta<0$, partial cancellation occurs in the region close to the molecular axis.

Another possible detachment orbital is the united atom (UA) orbital

$$f(r,\theta)=N\psi_d(r,\theta)\,, \tag{24}$$

where ψ_d is given by Eq. (23) and N normalizes $f(r,\theta)$ to unity outside the core region. We regard the overlapping spheres core region, and the LCAO detachment orbital given by Eqs. (17) and (18) to be the choices which are appropriate for the ZCC model. Most of our results will be obtained with them. They have the advantage that they will provide an easy method of constructing core shapes and detachment orbitals for multicentered ions. A few results will be obtained using the core shapes shown in Figs. 1(b) and 1(c), and the detachment orbitals of Eqs. (20) and (24), to explore the sensitivity of the model to these choices.

The final-state wave function ψ_k is chosen to be a plane wave as given in Eq. (12). The nature of the approximations inherent in using a plane-wave final state and a zero-core detachment orbital have been discussed in Ref. 1. When the matrix element $M_{k\lambda}(R,m)$ is evaluated at $R=R_{\nu'\nu''}$, it is consistent with the Franck-Condon principle to use the vertical detachment energy to determine the coefficient γ in the exponent in the detachment orbital

$$\gamma=\frac{(2m_e E_{\nu'\nu''})^{1/2}}{\hbar} \tag{25}$$

with $E_{\nu'\nu''}=E_{\nu'}-E_{\nu''}$, where $E_{\nu'}$ is the energy of the neutral molecule in the vibrational state ν' and electronic term A, and $E_{\nu''}$ is the energy of the ion in the vibrational state ν''. Similarly,

$$k=\frac{[2m_e(\hbar\omega-E_{\nu'\nu''})]^{1/2}}{\hbar}\,. \tag{26}$$

The function ψ_λ has a weak dependence on R through the coordinates r_A, θ_A, r_B, and θ_B, and the shape of the core region. However, $R_{\nu'\nu''}$ differs from the ion equilibrium internuclear distance r_e'' by less than 12% for the channels ($\nu'\leq 7$) considered. Thus, for simplicity, we will use r_e'' instead of $R_{\nu'\nu''}$ to determine r_A, θ_A, r_B, θ_B, and the core region.[18] The error in the total cross section, due to using r_e'', is less than 5% everywhere, and is less than 1% for energies at which four or more channels are open.

D. Computation of photodetachment quantities

The integration for the matrix element, Eq. (13), is most easily carried out using a molecular coor-

dinate system whose z axis passes through the two nuclei. However, the direction of the detached electron's momentum and the polarization of the incident light must be specified with respect to a laboratory frame of reference. We will choose the laboratory frame so that $\vec{k}$ is parallel to the z axis and $\hat{e}$ lies in the x-z plane. Its origin is at the midpoint of the internuclear axis. The molecular coordinate system can be obtained by rotating the laboratory coordinates through an angle α about the z axis, and then through an angle β about the new y axis. Thus α and β give the orientation of the molecule as in Fig. 2. The integration over the orientation of the molecule $d\Omega_m$ becomes an integration over $d\alpha \sin(\beta) d\beta$.

Using the wave functions of Eqs. (12) and (16), and using Euler's angles α and β to transform $\vec{k}$ and $\hat{e}$ into the molecular coordinate system, we obtain

$$\frac{1}{4\pi}\int |M_{\vec{k}\lambda}(R_{\nu'\nu''},\hat{m})|^2 d\alpha \sin\beta\, d\beta = \frac{1}{(2\pi)^2}(\tfrac{1}{2}C\cos^2\chi - \tfrac{1}{4}S\sin^2\chi), \quad (27)$$

where χ is the angle between $\vec{k}$ and $\hat{e}$:

$$C = \int [(I_0 - I_2)^{\frac{1}{2}}\sin\beta + I_1\cos\beta]^2 \sin\beta\, d\beta \quad (28)$$

and

$$S = \int \left(\frac{(I_0+I_2)^2}{4} + [(I_0 - I_2)^{\frac{1}{2}}\cos\beta - I_1\sin\beta]^2 \right) \times \sin\beta\, d\beta, \quad (29)$$

where

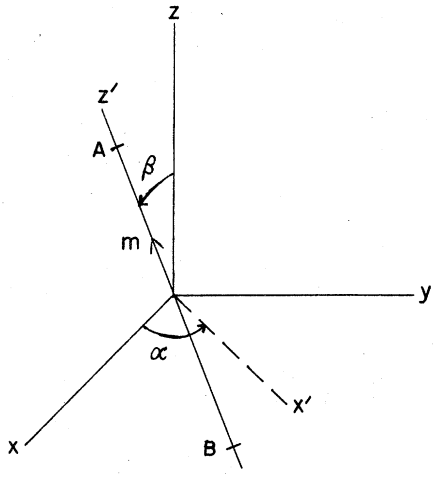

FIG. 2. Orientation of diatomic ion relative to laboratory frame of reference.

$$I_0 = \int\int \sin^2\theta \sin(kr\cos\beta\cos\theta) \times J_0(kr\sin\beta\sin\theta) f(r,\theta) r^3 dr\, d\theta, \quad (30)$$

$$I_1 = \int\int \sin\theta\cos\theta \sin(kr\cos\beta\cos\theta) \times J_1(kr\sin\beta\sin\theta) f(r,\theta) r^3 dr\, d\theta, \quad (31)$$

and

$$I_2 = \int\int \sin^2\theta \sin(kr\cos\beta\cos\theta) \times J_2(kr\sin\beta\sin\theta) f(r,\theta) r^3 dr\, d\theta. \quad (32)$$

In these integrals, J_i is the Bessel function of order i, and $f(r,\theta)$ is given by Eqs. (17), (20), or (24). In obtaining Eqs. (28) and (29), we have made use of the fact that $f(r,\pi-\theta) = -f(r,\theta)$, which is necessary for a π_g orbital. The integrals in Eqs. (30), (31), and (32) are over values of r and θ lying outside the core region. These integrals and the integrals over β in Eqs. (28) and (29) are carried out numerically. It should be noted that the integrals C and S depend on the initial and final vibrational states ν'' and ν' and the electronic term A.

Substituting into Eq. (14), the differential cross section is

$$\frac{d\sigma}{d\Omega}(A,\nu',\nu'') = F(\nu'\nu'')\frac{e^2}{\hbar c}\frac{m_e k\omega}{\hbar}\left|\langle A,\pi_g\}^2\Pi_g\rangle\right|^2 \times (\tfrac{1}{2}C\cos^2\chi + \tfrac{1}{4}S\sin^2\chi). \quad (33)$$

The partial cross section for detachment via a specific channel, with the electron's momentum in any direction is

$$\sigma(A,\nu',\nu'') = 2\pi\int \frac{d\sigma}{d\Omega}\sin\chi\, d\chi = F(\nu',\nu'')\frac{2\pi}{3}\frac{e^2}{\hbar c}\frac{m_e k\omega}{\hbar}\left|\langle A,\pi_g\}^2\Pi_g\rangle\right|^2 (C+S). \quad (34)$$

Because we have averaged over all orientations of the ion, the differential cross section can be written in the form[19]

$$\frac{d\sigma}{d\Omega}(A,\nu',\nu'') = \frac{\sigma(A,\nu',\nu'')}{4\pi} \times [1+\beta(A,\nu',\nu'')(\tfrac{3}{2}\cos^2\chi + \tfrac{1}{2})]. \quad (35)$$

Rearrangement of Eq. (33) gives

$$\beta(A,\nu',\nu'') = \frac{2C-S}{C+S}. \quad (36)$$

Many photodetachment experiments do not distinguish electrons detached through different vibrational and electronic channels. The total photodetachment cross section measured by such ex-

periments corresponds to

$$\sigma_0 = \sum_{\nu''} P(\nu'') \sum_A \sum_{\nu'} \sigma(A, \nu', \nu''). \quad (37)$$

The summations extend over values of A and ν' such that $E_{\nu'\nu''} < \hbar\omega$. $P(\nu'')$ is the probability of finding the ion in the initial vibrational state ν''. In an experiment in which the ions are allowed to relax to their ground vibrational state, such as those employing drift tubes, $P(0) = 1$ and $P(\nu'') = 0$ for $\nu'' > 0$.

III. RESULTS AND COMPARISON WITH PHOTODETACHMENT EXPERIMENTS

In this section we compare the results of the analysis of Sec. II with experiments for O_2^- and S_2^-. The parameters employed for these ions are given in Table I. $\hbar\omega_e$, $\hbar\omega_e x_e$, $\hbar\omega_e y_e$, and $\hbar\omega_e z_e$ are constants which give the vibrational energy spectrum as defined by Herzberg[21]:

$$E_\nu = \hbar\omega_e(\nu+\tfrac{1}{2}) - \hbar\omega_e x_e(\nu+\tfrac{1}{2})^2 + \hbar\omega_e y_e(\nu+\tfrac{1}{2})^3 + \hbar\omega_e z_e(\nu+\tfrac{1}{2})^4, \quad (38)$$

where E_ν is the vibrational energy eigenvalue. These constants are used to determine the vibrational energy differences $E_{\nu'\nu''}$.

For computing the Franck-Condon factors, Morse potentials have been used to describe the vibrational motion of O_2, S_2, and O_2^-. The Morse potential parameters[21] have been determined using the values of $\hbar\omega_e$ and $\hbar\omega_e x_e$. For S_2^- we have used an harmonic-oscillator potential, since no value of $\hbar\omega_e x_e$ is known. r_e'' and r_e' are also needed to determine the internuclear potentials. The results quoted in Secs. III A, III B, and III C are computed using an overlapping spheres core [Fig. 1(a)] and LCAO detachment orbital [Eqs. (17) and (18)]. Other core shapes and detachment orbitals are considered in Sec. III D.

A. The total photodetachment cross section

The total photodetachment cross section is the sum of partial cross sections for many vibrational channels as indicated in Eq. (37). This is illustrated in Fig. 3, which shows the sums for the first few vibrational channels of the $^3\Sigma_g^-$ term of the molecule, with the ion initially in the $\nu'' = 0$ vibrational state. Channels with ν' greater than seven make an insignificant contribution to the total cross section.

Figure 4 shows the total cross section calculated by the ZCC model, for channels ending in all vibrational states and the $^3\Sigma_g^-$, $^1\Delta_g$, and $^1\Sigma_g^+$ electronic terms of the molecule. It is assumed that only the ground vibrational state ($\nu'' = 0$) is populated.

TABLE I. Parameters for the calculation of photodetachment quantities.

		O_2^- $^3\Sigma_g^-$	O_2^- $^1\Delta_g$	O_2^- $^1\Sigma_g^+$	S_2^- $^3\Sigma_g^-$
$E_{0\,0}$	(eV)	0.44[a]	1.447[e]	2.097[e]	1.663[f]
r_0	(Å)	0.96[b]	0.96[b]	0.96[b]	1.51[b]
r_e'	(Å)	1.207[c]	1.2155[c]	1.227[c]	1.889[c]
r_e''	(Å)	1.341[a]	1.341[a]	1.341[a]	2.004[g]
$\hbar\omega_e'$	(eV)	0.1959[c]	0.187[c]	0.1776[c]	0.0899[c]
$\hbar\omega_e x_e'$	(eV)	1.50×10^{-3}[c]	1.48×10^{-3}[c]	1.7×10^{-3}[c]	3.53×10^{-4}[c]
$\hbar\omega_e y_e'$	(eV)	6.77×10^{-6}[c]		-1.33×10^{-6}[c]	
$\hbar\omega_e z_e'$	(eV)	-1.8×10^{-7}[c]			
$\hbar\omega_e''$	(eV)	0.135[d]	0.135[d]	0.135[d]	0.065[f]
$\hbar\omega_e x_e''$	(eV)	1.5×10^{-3}[d]	1.5×10^{-3}[d]	1.5×10^{-3}[d]	
$\langle A, \pi_g\}^2 \Pi_g\rangle$		0.500[h]	0.333[h]	0.167[h]	0.500[h]

[a] Reference 7.
[b] Calculated from Eq. (15) with $\langle r^2\rangle$ from Ref. 20.
[c] Reference 21.
[d] Reference 22.
[e] Obtained by combining energies for the excited electronic term (given in Ref. 21) with the electron affinity from Ref. 7.
[f] Reference 8.
[g] Obtained by fitting ratios of partial cross sections given by Ref. 8.
[h] Obtained from formulas of Ref. 16.

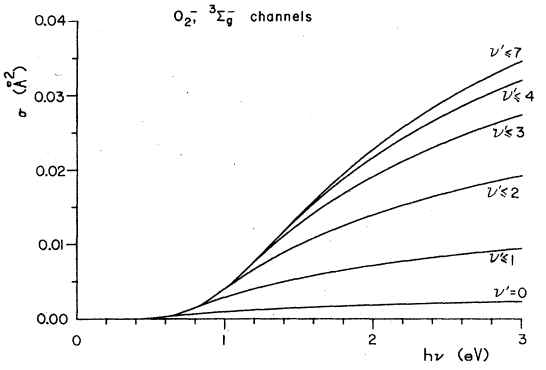

FIG. 3. The calculated cross section of O_2^- for channels ending in the $^3\Sigma_g^-$ term. The curves show the sums of the partial cross sections for the first few vibrational channels as indicated. Only the lowest vibrational state of the ion is occupied.

In addition, the sum of the partial cross sections for channels ending in only the $^3\Sigma_g^-$ molecular term (the ground electronic state), and the sums for channels ending in the $^3\Sigma_g^-$ and $^1\Delta_g$ terms are shown. For comparison, the cross section measured by Burch, Smith, and Branscomb[23] is shown as the dashed line in Fig. 4. The isolated points show measurements by Cosby *et al.*[4]

It can be seen that the shape of the ZCC cross section generally agrees with the experimentally measured one. However, the ZCC cross section is uniformly too large by a factor of about 2, except at photon energies less than 1 eV. This lies outside the experimental uncertainty of 14% in the absolute normalization of the cross section quoted by Ref. 2, and the experimental uncertainty of 12% in the absolute normalization quoted by Ref. 4. Both the experimental and the calculated total cross sections increase, with increasing slope, as the photon energy increases. It should be noted that this behavior results from the opening of new channels as the photon energy increases.

The Burch, Smith, and Branscomb data may represent detachment for which at least some of the ions are in an excited vibrational state, since the data are best fit by a threshold energy of 0.15 eV. Figure 5 shows the total cross section which results assuming the ion vibrational states $\nu'' = 0$, 1, 2, and 3 have populations corresponding to a temperature of 1500 K. In that figure, it can be seen that the ZCC cross section remains larger than the experimental cross section at all energies. At photon energies greater than 1 eV, this cross section is nearly identical to the theoretical cross section shown in Fig. 4, indicating that the population of excited vibrational states of the ion has little effect on the total cross section, except near threshold.

The cross section predicted by the ZCC model, with the parameters of Table I for S_2^-, is displayed in Fig. 6. We have included only the $^3\Sigma_g^-$ molecular term and assumed that all the ions are in the $\nu'' = 0$ state. To our knowledge, the total photodetachment cross section of S_2^- has not been measured.

B. Relative partial cross sections

Table II(a) compares the ratios of partial cross sections obtained in an LPES experiment[7] on O_2^-

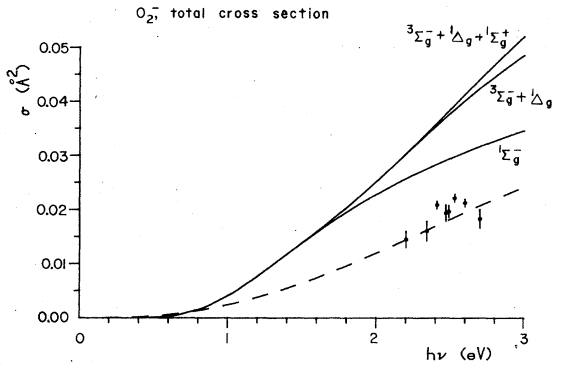

FIG. 4. Total O_2^- photodetachment cross section. The upper solid curve shows the total cross section calculated by the ZCC model for all channels leaving the molecule in the $^3\Sigma_g^-$, $^1\Delta_g$, or $^1\Sigma_g^+$ electronic term. The middle solid curves show the sums of the cross sections for all channels ending in the lower electronic terms as indicated. Only the lowest vibrational state of the ion is occupied. The dashed line shows the experimental data of Ref. 2. The points indicated ϕ are data from Ref. 4.

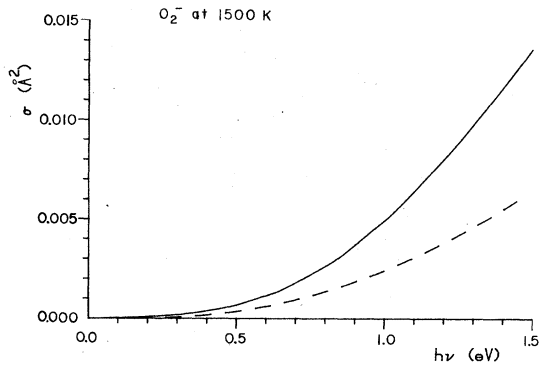

FIG. 5. Total O_2^- photodetachment cross section at 1500 K. The solid line is the total cross section computed by the ZCC model for all channels ending in the $^3\Sigma_g^-$, $^1\Delta_g$, and $^1\Sigma_g^+$ electronic terms. The vibrational levels of the ion have been assigned the populations $P(0) = 0.648$, $P(1) = 0.233$, $P(2) = 0.086$, and $P(3) = 0.032$, which correspond to a Boltzmann distribution with a temperature of 1500 K. The dashed line represents the data of Ref. 2.

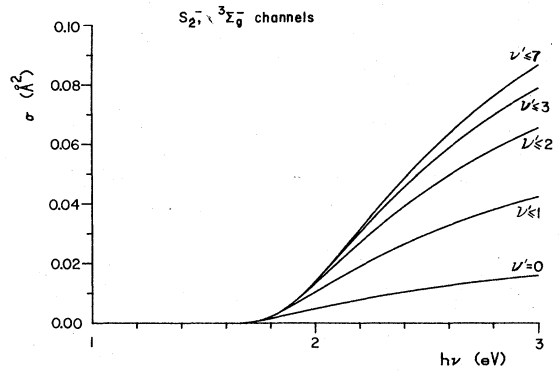

FIG. 6. S_2^- photodetachment cross section. The curve shows the total cross section computed by the ZCC model for channels ending in the $^3\Sigma_g^-$ term of S_2^-. Only the lowest vibrational state of the ion is occupied.

at a photon energy of 2.54 eV, and ratios obtained by the ZCC model using two different values for r_e'', 1.341 and 1.348 Å. The value $r_e''=1.341$ Å was obtained in Ref. 7 by adjusting r_e'' so that the ratios of the Franck-Condon factors best fit the experimental ratios. This amounts to assuming the electronic contribution to the cross section, the quantity which multiplies the Franck-Condon factor on the right-hand side of Eq. (34), is constant for $1<\nu'<4$. The ZCC model enables one to account for the difference in the electronic contribution for different vibrational transitions. Using the ZCC model to compute the electronic contribution, the best least-squares fit which can be obtained by varying r_e'', while keeping all other parameters as given in Table I, is $r_e''=1.348$ Å. The difference in the two values for r_e'' reflects the fact that the electronic contribution for $\nu'=4$ is only 70% as large as that for $\nu'=1$, for a photon energy $\hbar\omega=2.54$ eV.[24] An uncertainty of ±0.01 Å is placed on the value of r_e'' in Ref. 7. The value we have obtained here lies within this uncertainty. However, the quoted uncertainty is, in part, due to the uncertainty of the assumption that the electronic contribution is the same for all vibrational channels. Use of the ZCC model to determine this contribution can reduce the uncertainty in the determina-

TABLE II. Comparison of partial cross-section ratios at $\hbar\omega=2.54$ eV.

(a) O_2^-

	ZCC $r_e''=1.341$ Å	ZCC $r_e''=1.348$ Å	Experimental Ref. 7
$\frac{\sigma(^3\Sigma_g^-,1,0)}{\sigma(^3\Sigma_g^-,2,0)}$	0.744	0.665	0.6409 ± 0.019
$\frac{\sigma(^3\Sigma_g^-,2,0)}{\sigma(^3\Sigma_g^-,3,0)}$	1.230	1.101	1.100 ± 0.033
$\frac{\sigma(^3\Sigma_g^-,3,0)}{\sigma(^3\Sigma_g^-,4,0)}$	1.832	1.646	1.673 ± 0.050

(b) S_2^-

$\chi=90°$	ZCC $r_e''=2.004$ Å	Experimental Ref. 9
$\frac{d\sigma}{d\Omega}(^3\Sigma_g^-,0,0)$ / $\frac{d\sigma}{d\Omega}(^3\Sigma_g^-,1,0)$	0.62	0.78
$\frac{d\sigma}{d\Omega}(^3\Sigma_g^-,1,0)$ / $\frac{d\sigma}{d\Omega}(^3\Sigma_g^-,2,0)$	1.18	1.14
$\frac{d\sigma}{d\Omega}(^3\Sigma_g^-,2,0)$ / $\frac{d\sigma}{d\Omega}(^3\Sigma_g^-,3,0)$	1.81	1.60

tion of r_e''.

Badger's rule is an empirical rule which relates the vibrational frequency ω_e'' and the internuclear distance r_e'' for molecules composed of atoms in the first two rows of the periodic table. This rule is[21]

$$\mu\omega_e''^2(r_e''-d)^3=C\,, \tag{39}$$

where μ is the reduced mass. C and d are constants for all molecules with atoms from the same row of the periodic table. For a molecule with both atoms from the first row $d=0.68$ Å, and if both atoms are in the second row $d=1.25$ Å. In both cases $C=1.86$ Å^{3}N/cm. For O_2^-, with $h\omega_e''=0.135$ eV, this rule predicts $r_e''=1.372$ Å. The value that we have obtained lies between this value and the value obtained ignoring the variation in the electronic contribution as in Ref. 7.

Table II(b) shows calculated and experimental ratios for S_2^-. Again the experimental ratios are obtained in an LPES experiment[8] at a photon energy of 2.54 eV. These experimental ratios are the ratios of the electron flux measured perpendicular to the polarization of the incident photons. Thus these ratios correspond to ratios of the differential cross sections $(d\sigma/d\Omega)(^3\Sigma_g^-,\nu',0)$ at $\chi=90°$. The corresponding theoretical ratios are calculated using Eq. (35), with values of β given by Eq. (36).

The best fit to the experimental ratios occurs for $r_e''=2.004$ Å. It should be noted that the experimental ratios were estimated from peak heights in data provided by Ref. 8. No attempt was made to obtain the areas under the peaks by fitting Gaussian distributions to them, nor has any correction been made for background present in the data. Badger's rule yields $r_e''=2.144$ Å for $h\omega_e''=0.065$ eV. The value obtained using the ZCC model lies 7% below this.

C. Angular distribution of photodetached electrons

The angular distribution of photodetached electrons is specified by the anisotropy parameter $\beta(A,\nu',\nu'')$ which can be calculated using Eq. (36). The resulting values of $\beta(^3\Sigma_g,\nu',0)$ are shown in Fig. 7(a) for O_2^- and in Fig. 7(b) for S_2^-. Note that β depends upon the vibrational channel as well as the electron kinetic energy. These figures show that for both O_2^- and S_2^-, $\beta=+0.2$ at the threshold for all channels, and decreases towards -1 as the electron kinetic energy increases. For kinetic energies above 0.5 eV, these curves imply that the maximum flux of detached electrons emerges perpendicular to the polarization of the incident light.

The anisotropy parameter β has been measured[7] for O_2^-. The measurement was done at a single photon energy (2.54 eV), but the angular distributions of electrons detached via several channels was observed. Table III compares these experimental results with the results of our calculations. The calculations of the anisotropy parameters given here are, to our knowledge, the first computations of β for individual vibrational transitions.

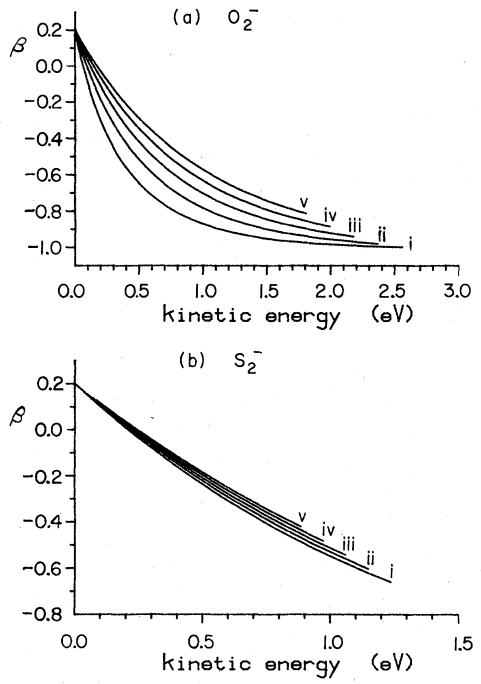

FIG. 7. Angular distribution of photoelectrons for O_2^- and S_2^-. The curves show the values calculated by the ZCC model for the anisotropy parameter of individual vibrational channels; (i) Represents $\beta(^3\Sigma_g^-,0,0)$, (ii) represents $\beta(^3\Sigma_g^-,1,0)$, (iii) represents $\beta(^3\Sigma_g^-,2,0)$, (iv) represents $\beta(^3\Sigma_g^-,3,0)$, and (v) represents $\beta(^3\Sigma_g^-,4,0)$.

D. Alternative choices of core shape and detachment orbital

The effects of altering the core shape and detachment orbital are illustrated by the results giv-

TABLE III. Anisotropy factors at $\hbar\omega=2.54$ eV.

	ZCC	Experimental Ref. 7
$\beta(^3\Sigma_g^-,1,0)$	−0.949	−0.9492 ± 0.005
$\beta(^3\Sigma_g^-,2,0)$	−0.884	−1.000 ± 0.01
$\beta(^3\Sigma_g^-,3,0)$	−0.800	−0.8880 ± 0.0053
$\beta(^3\Sigma_g^-,4,0)$	−0.699	−0.7865 ± 0.0066
$\beta(^1\Delta_g,1,0)$	−0.418	−0.45 ± 0.02
$\beta(^1\Delta_g,2,0)$	−0.292	−0.41 ± 0.05
$\beta(^1\Delta_g,3,0)$	−0.168	−0.22 ± 0.08

en in Table IV. We have tabulated the total absolute cross sections, the ratios of partial cross sections, and the anisotropy parameters β at a photon energy of 2.54 eV, for the various core shapes and detachment orbitals discussed in Sec. II. Of these quantities, the absolute total cross section is the most strongly affected. Taking as a nominal value the cross section for the overlapping spheres core and LCAO detachment orbital, the total cross section varies from 1.7 times the nominal value for the ellipsoidal core, to 0.425 of the nominal value for the mixed LCAO orbital with $\delta = -0.5$. Note that $\delta = -0.5$ corresponds to approximately 25% d-atomic orbital in the linear combination. The shape of the graphs of the total cross section as a function of energy are nearly the same for all the choices of core shape and detachment orbital.

The absolute cross section obtained using the UA orbital of Eq. (24) can be seen to be in better agreement with the experimental results than is the result obtained using the LCAO orbital. However, the UA orbital has a very strong singularity at the midpoint of the internuclear axis. Use of the overlapping spheres core region with this orbital results in a normalization constant which is unrealistically small.

The ratios of partial cross sections vary by no more than 2% from the nominal values, and the anisotropy parameters vary by no more than 5% from the nominal values. Overall, we can conclude that the details of the shape of the core region and the detachment orbital can alter the absolute size of the cross section somewhat, but have very little significance for either the shape of the cross section as a function of energy, or the other photodetachment quantities. The essential feature that the detachment orbital must have, regardless of what other choices are made, is the correct asymptotic behavior outside the core region.

IV. CONCLUSIONS

We have applied the ZCC model to computation of the photodetachment quantities of O_2^- and S_2^-. The model yields a total absolute cross section for O_2^- which is about twice as large as the measured cross section. However, the quantities that do not depend on the absolute normalization, namely, the shape of the total cross section, the ratios of partial cross sections, and the anisotropy parameters, agree with experimental results within a few percent.

The absolute cross sections are sensitive to the choice of the core radius r_0. The choice that we have made for this parameter in this article coincides with the choice that was made for atomic ions.[1] It is possible that investigation of additional molecular ions using the ZCC model will reveal a method of choosing r_0 that will improve the certainty with which absolute cross sections for molecular ions are calculated. These calculations for O_2^- and S_2^- are illustrative of many of the facets of the calculation of photodetachment cross sections for other molecular negative ions. In particular, the incorporation of vibrational as well as electronic effects is very useful. For example, the ability to compute the partial cross sections for vibrational channels allows us to investigate the effect that population of excited ionic vibra-

TABLE IV. Comparison of photodetachment quantities for various choices of core shape and detachment orbital at 2.54 eV. σ_0 is the total cross section, $\rho(\mu\nu) = \sigma(^3\Sigma_g^-, \mu, 0)/\sigma(^3\Sigma_g^-, \nu, 0)$, and $\beta(^3\Sigma_g^-, \nu, 0)$ is the anisotropy parameter defined in Eq. (36). The combinations of core shape and detachment orbital are (a) LCAO orbital, overlapping spheres core; (b) LCAO orbital, oval core; (c) LCAO orbital, ellipsoidal core; (d) mixed LCAO orbital with $\delta = +0.5$, overlapping spheres core; (e) mixed LCAO orbital with $\delta = -0.5$, overlapping spheres core; (f) UA orbital, overlapping spheres core; and (g) experimental, with total cross section from Ref. 2, the remaining quantities from Ref. 7.

	(a)	(b)	(c)	(d)	(e)	(f)	(g)
$\sigma_0(\text{Å}^2)$	0.040	0.041	0.068	0.044	0.017	0.028	0.019
$\rho(1,2)$	0.74	0.74	0.73	0.74	0.76	0.75	0.64
$\rho(2,3)$	1.23	1.23	1.22	1.23	1.25	1.24	1.10
$\rho(3,4)$	1.83	1.83	1.80	1.83	1.85	1.84	1.67
$\beta(^3\Sigma_g^-, 1, 0)$	−0.95	−0.95	−0.97	−0.95	−0.93	−0.94	−0.95
$\beta(^3\Sigma_g^-, 2, 0)$	−0.88	−0.89	−0.91	−0.89	−0.86	−0.88	−1.00
$\beta(^3\Sigma_g^-, 3, 0)$	−0.80	−0.80	−0.83	−0.81	−0.78	−0.79	−0.89
$\beta(^3\Sigma_g^-, 4, 0)$	−0.70	−0.70	−0.73	−0.71	−0.68	−0.69	−0.79

tional states (hence, ion temperature) has on the apparent photodetachment cross section. We find that the ion temperature has an insignificant effect except at photon energies below 1 eV, for O_2^-. Since vibrational excitation of the ion can be incorporated in the model, it will be possible to compute the solar detachment rate as a function of temperature.

The ability of the ZCC model to compute partial cross sections for vibrational channels, and to give information about the angular distribution, makes it a valuable aid in the analysis of experimental photodetachment data. For example, a recent experimental investigation[25] of NO_2^- reveals a series of thresholds in the cross section corresponding to the opening of additional vibrational channels as the photon energy increases. The ZCC model can provide a reliable estimate of the electronic cross section for each channel. Such estimates are useful in order to infer structural and spectral constants from experimental data.

The results given here for O_2^- and S_2^- demonstrate that the ZCC model can be applied to homonuclear diatomic ions. Future work will apply the ZCC model to heteronuclear diatomic, triatomic, and tetratomic anions. The simplicity of the model as applied to homonuclear diatomic ions indicates that it will yield useful results for these more complicated anions.

ACKNOWLEDGMENTS

We wish to acknowledge helpful discussions with Dr. R. N. Hill. This work was supported in part by NSF Grant No. ATM-77-18324.

[1]R. M. Stehman and S. B. Woo, Phys. Rev. A 20, 281 (1979).
[2]D. S. Burch, S. J. Smith, and L. M. Branscomb, Phys. Rev. 112, 171 (1958).
[3]P. Warneck, GCA Technical Report No. 69-13-N, GCA Corporation, Bedford, Mass. (unpublished).
[4]P. C. Cosby, R. A. Bennett, J. R. Peterson, and J. T. Moseley, J. Chem. Phys. 63, 1612 (1975).
[5]R. A. Beyer and J. A. Vanderhoff, BRL Report No. 1922, Ballistic Research Laboratories, Aberdeen Proving Ground, Maryland (unpublished).
[6]S. B. Woo, L. M. Branscomb, and E. C. Beaty, J. Geophys. Res. 74, 2933 (1969).
[7]R. J. Celotta, R. A. Bennett, J. L. Hall, M. W. Siegal, and J. Levine, Phys. Rev. A 6, 631 (1972).
[8]R. J. Celotta, R. A. Bennett, and J. L. Hall, J. Chem. Phys. 60, 1740 (1974).
[9]S. Geltman, Phys. Rev. 112, 176 (1958).
[10]K. J. Reed, A. H. Zimmerman, H. C. Anderson, and J. I. Brauman, J. Chem. Phys. 64, 1368 (1976).
[11]R. S. Mulliken, Rev. Mod. Phys. 4, 1 (1932).
[12]It should be noted that the selection rule, $\Delta J = \pm 1, 0$, limits the amount of energy absorbed or given up by changes in the rotational state to about 0.01 eV. Our results, therefore, represent cross sections measured with a resolution no better than about 0.01 eV.
[13]The expansion in powers of $R - \bar{R}$ is actually an expansion in the $\frac{1}{4}$th power of the unitless quantity (m_e/M) [cf. M. Born and K. Huang, *Dynamical Theory of Crystal Lattices* (Oxford University Press, London, 1962), p. 166ff]. Thus, ignoring terms of order $(R-\bar{R})^2$ amounts to ignoring terms of order $(m_e/M)^{1/2} \approx \frac{1}{100}$.
[14]P. H. Krupenie, J. Phys. Chem. Ref. Data 1, 423 (1972).
[15]R. M. Stehman, Ph.D. dissertation, University of Delaware, 1980 (unpublished).
[16]J. S. Griffith, *The Irreducible Tensor Method for Molecular Symmetry Groups* (Prentice-Hall, Englewood Cliffs, N.J., 1962).
[17]J. C. Slater, *Quantum Theory of Molecules and Solids* (McGraw-Hill, New York, 1963), Vol. 1.
[18]This causes less than 6% error in the partial cross sections, except for the channels with $\nu' = 6$ and 7. For these channels the errors reach 12%, but the Franck-Condon factors for these transitions are very small. When the partial cross sections are added together the errors tend to cancel.
[19]J. C. Tully, R. S. Berry, and B. J. Dalton, Phys. Rev. 176, 95 (1968).
[20]C. C. Lu, T. A. Carlson, F. B. Malik, T. C. Tucker, and C. W. Nestor, Jr., At. Data 3, 1 (1971).
[21]G. Herzberg, *Molecular Spectra and Molecular Structure* (Van Nostrand, New York, 1950), Vol. 1.
[22]M. J. Boness and G. J. Schulz, Phys. Rev. A 2, 2182 (1970).
[23]The experimental values quoted from Burch, Smith, and Branscomb (Ref. 2) are values calculated from their Eq. (2), which they use to fit their experimental data.
[24]Reference 7 employs an accurate Rees, Klein, and Rydberg (RKR) potential to describe the vibrational motion of the molecule. However, if the ratios are fit using the Morse potential, but assuming the electronic contribution to be constant, the best fit is obtained for $r_e'' = 1.342$ Å, only 0.001 Å different than obtained in Ref. 7.
[25]S. B. Woo, E. M. Helmy, P. H. Mauk, and A. P. Paszek (unpublished).